

## Structural and Magnetic Properties of Three One-Dimensional Azido-Bridged Copper(II) and Manganese(II) Coordination Polymers

En-Qing Gao,<sup>†,‡,§</sup> Shi-Qiang Bai,<sup>†,‡</sup> Chuan-Feng Wang,<sup>‡</sup> Yan-Feng Yue,<sup>‡</sup> and Chun-Hua Yan<sup>\*,†</sup>

State Key Laboratory of Rare Earth Materials Chemistry and Applications & PKU–HKU Joint Laboratory on Rare Earth Materials and Bioinorganic Chemistry, Peking University, Beijing 100871, China, Department of Chemistry, Qufu Normal University, Qufu 273165, Shandong, China, and Shanghai Key Laboratory of Green Chemistry and Chemical Processes, East-China Normal University, Shanghai 200062, China

Received June 4, 2003

Three one-dimensional (1D) azido-bridged coordination polymers of formula  $[\text{Cu}(\text{L})(\text{N}_3)_2]_n$  (**1**),  $[\text{Cu}_2(\text{Me-L})(\text{N}_3)_4]_n$  (**2**), and  $[\text{Mn}(\text{L})(\text{N}_3)_2]_n$  (**3**) have been synthesized and structurally characterized, and their magnetic properties studied, where L and Me-L are 2-(pyrazol-1-ylmethyl)pyridine and 2-(3-methylpyrazol-1-ylmethyl)pyridine, respectively. Compound **1** consists of 1D chains in which the Cu(II) ions with a square pyramidal geometry are alternately bridged by an end-to-end (EE) and an end-on (EO) azido ligands, both adopting a basal–apical disposition. Compound **2** exhibits an unprecedented chain topology built via three different kinds of EO azido bridges. Four Cu(II) ions in the square pyramidal environment are alternately bridged by single and double EO bridges to form a tetranuclear cyclic ring, and neighboring rings are interlinked by double EO bridges to generate a “chain of rings”. The intraannular double azido ions are disposed between metal ions in a basal–basal fashion, and the other two kinds of azido ions adopt the basal–apical disposition. Compound **3** consists of 1D concavo–convex chains in which cis-octahedrally coordinated Mn(II) ions are alternately bridged by double EE and double EO bridges. There exist  $\pi$ – $\pi$  interactions between the ligands bound to the neighboring Mn(II) ions bridged by the EO bridges. Temperature- and field-dependent magnetic analyses reveal alternate ferromagnetic interactions for **1**, dominating ferromagnetic interactions for **2**, and alternating ferro- and antiferromagnetic interactions through the EO and EE azido bridges for **3**, respectively.

## Introduction

The design and magnetism of discrete polynuclear molecules and coordination polymers of paramagnetic metal ions are currently of considerable interest, for understanding the fundamental science of magnetic interactions and magneto-structural correlations in molecular systems, and for developing new functional molecule-based materials.<sup>1,2</sup> In this context, azido-bridged complexes have received intense attention due to the remarkable diversities of the complexes in structure and in magnetism.<sup>3</sup> The azido ion can link metal ions in  $\mu$ -1,1 (end-on, EO),  $\mu$ -1,3 (end-to-end, EE),  $\mu$ -1,1,3, or still other modes (Scheme 1), yielding various polynuclear,

one-, two-, or three-dimensional species with specific topologies.<sup>3–5</sup> The magnetic exchange mediated via an azido bridge can be ferro- (F) or antiferromagnetic (AF), dependent on the bridging mode and bonding parameters. For instance, it has been widely stated that the exchange is generally ferromagnetic for the EO mode and antiferromagnetic for the EE mode, but an increasing number of exceptions have been reported recently. Furthermore, different bridging modes of the azido ions may simultaneously exist in the same

\* To whom correspondence should be addressed. Fax: +86-10-62754179. E-mail: chyan@chem.pku.edu.cn.

<sup>†</sup> Peking University.

<sup>‡</sup> Qufu Normal University.

<sup>§</sup> East-China Normal University.

(1) Kahn, O. *Molecular Magnetism*; VCH: New York, 1993.

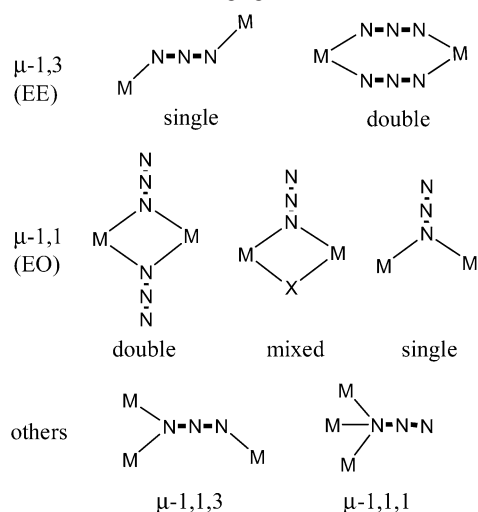
(2) *Magnetism: Molecules to Materials*; Miller, J. S.; Drilon, M., Eds.; Wiley-VCH: Weinheim, 2002.

(3) Ribas, J.; Escuer, A.; Monfort, M.; Vicente, R.; Cortés, R.; Lezama, L.; Rojo, T. *Coord. Chem. Rev.* **1999**, 193–195, 1027 and references therein.

(4) (a) Serna, Z. E.; Lezama, L.; Urtiaga, M. K.; Arriortua, M. I.; Barandika, M. G. B.; Cortés, R.; Rojo, T. *Angew. Chem., Int. Ed.* **2000**, 39, 344. (b) Goher, M. A. S.; Cano, J.; Journaux, Y.; Abu-Youssef, M. A. M.; Mautner, F. A.; Escuer, A.; Vicente, R. *Chem. Eur. J.* **2000**, 6, 778.

(5) (a) Meyer, F.; Kircher, P.; Pritzkow, H. *Chem. Commun.* **2003**, 774. (b) Guo, G.-C.; Mak, T. C. W. *Angew. Chem., Int. Ed.* **1998**, 37, 3286. (c) Papaefstathiou, G. S.; Perlepes, S. P.; Escuer, A.; Vicente, R.; Font-Bardia, M.; Solans, X. *Angew. Chem., Int. Ed.* **2001**, 40, 884.

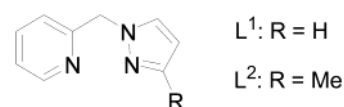
Scheme 1. Selected Azido Bridging Modes



species, leading to novel topologies and magnetic behaviors that may be difficult to achieve with other bridging ligands.<sup>6–11</sup> For copper(II) species, the situation is further complicated by the variety of the metal ion in coordination number and geometry.<sup>12–15</sup>

On the other hand, the EO azido bridge tends to coexist with another azido bridge (EO or EE) or other bridging groups, such as carboxylato and diazine<sup>16,17</sup> The occurrence of the EO bridge as the only bridge between two metal ions is very rare. To our knowledge, only one compound has been

Chart 1



reported to contain this type of EO azido bridge.<sup>18</sup> The compound,  $[\text{CuL}'(\text{N}_3)_2]_n$  (**4**,  $\text{L}' = \text{homopiperazine}$ ), reported by Chaudhuri et al. in 2000, consists of one-dimensional (1D) antiferromagnetic Cu(II) chains with alternate single end-on and single end-to-end azido bridges. In this paper, we report the syntheses, structures, and magnetic properties of two new 1D azido-bridged Cu(II) compounds (**1** and **2**) with 2-(pyrazol-1-ylmethyl)pyridine (L, Chart 1) and 2-(3-methylpyrazol-1-ylmethyl)pyridine (Me-L). A manganese(II)–azido complex (**3**) with the L ligand is also reported. Compounds **1** and **2** represent new examples of metal complexes containing single EO azido bridges, but they exhibit completely different polymeric topologies. Compound **1**, of formula  $[\text{CuL}(\text{N}_3)_2]_n$ , also consists of 1D chains with alternate single EE and single EO azido bridges, but the magnetic interactions mediated by the bridges are opposite to those in **4**. Compound **2**, of formula  $[\text{Cu}_2(\text{Me-L})(\text{N}_3)_4]_n$ , exhibits an unprecedented chain topology, which is achieved via three different types of EO azido bridges. Complex **3**, of formula  $[\text{MnL}(\text{N}_3)_2]_n$ , consists of 1D chains with alternating F and AF interactions through double EO and double EE azido bridges, respectively.

## Experimental Section

**Materials and Synthesis.** All the starting chemicals were of AR grade and used as received. The L and Me-L ligands were prepared according to the literature methods.<sup>19</sup>

**CAUTION!** Although not encountered in our experiments, perchlorate and azido complexes of metal ions are potentially explosive. Only a small amount of the materials should be prepared, and it should be handled with care.

**$[\text{CuL}(\text{N}_3)_2]_n$  (**1**).** A methanol solution (10 mL) containing  $\text{Cu}(\text{ClO}_4)_2 \cdot 6\text{H}_2\text{O}$  (0.50 mmol) and L (0.50 mmol) and the solution of  $\text{NaN}_3$  (1.0 mmol) in the same solvent (10 mL) were added into, respectively, the two arms of a H-shaped tube, and then about 15 mL of methanol was carefully added so that the bridge of the tube was filled. The tube was sealed and left to stand at room temperature. Slow diffusion between the two solutions afforded dark green crystals of **1** within 4 weeks. Yield, 64%. Anal. Calcd for  $\text{C}_9\text{H}_9\text{CuN}_9$ : C 35.24, H 2.96, N 41.09. Found: C 34.98, H 2.97, N 40.79%. Main IR ( $\text{cm}^{-1}$ ): 2064vs, 2038vs, 1606m, 1412m, 1310m, 1281m, 1022m, 996m, 763m. We have attempted to synthesize this compound by mixing the reactants in methanol directly: a methanolic solution (10 mL) containing sodium azide (1.0 mmol) was added with continuous stirring to a mixture solution of L (0.50

- (6) Gao, E.-Q.; Bai, S.-Q.; Yue, Y.-F.; Wang, Z.-M.; Yan, C.-H. *Inorg. Chem.* **2003**, *42*, 3642 and references therein.
- (7) (a) Cortés, R.; Drillon, M.; Solans, X.; Lezama, L.; Rojo, T. *Inorg. Chem.* **1997**, *36*, 677. (b) Abu-Youssef, M. A.; Escuer, A.; Gatteschi, D.; Goher, M. A. S.; Mautner, F. A.; Vicente, R. *Inorg. Chem.* **1999**, *38*, 5716.
- (8) (a) Abu-Youssef, M.; Escuer, A.; Goher, M. A. S.; Mautner, F. A.; Vicente, R. *Eur. J. Inorg. Chem.* **1999**, 687. (b) Villanueva, M.; Mesa, J. L.; Urriaga, M. K.; Cortés, R.; Lezama, L.; Arriortua, M. I.; Rojo, T. *Eur. J. Inorg. Chem.* **2001**, 1581.
- (9) (a) Escuer, A.; Cano, J.; Goher, M. A. S.; Journaux, Y.; Lloret, F.; Mautner, F. A.; Vicente, R. *Inorg. Chem.* **2000**, *39*, 4688. (b) Gao, E.-Q.; Bai, S.-Q.; Wang, Z.-M.; Yan, C.-H. *J. Am. Chem. Soc.* **2003**, *125*, 4984.
- (10) (a) Abu-Youssef, M.; Escuer, A.; Goher, M. A. S.; Mautner, F. A.; Reiss, G.; Vicente, R. *Angew. Chem., Int. Ed.* **2000**, *39*, 1624. (b) Abu-Youssef, M. A. M.; Drillon, M.; Escuer, A.; Goher, M. A. S.; Mautner, F. A.; Vicente, R. *Inorg. Chem.* **2000**, *39*, 5022.
- (11) (a) Ribas, J.; Monfort, M.; Resino, I.; Solans, X.; Rabu, P.; Maingot, F.; Drillon, M. *Angew. Chem., Int. Ed. Engl.* **1996**, *35*, 2520. (b) Escuer, A.; Vicente, R.; El Fallah, M. S.; Goher, M. A. S.; Mautner, F. A. *Inorg. Chem.* **1998**, *37*, 4466.
- (12) (a) Shen, Z.; Zuo, J. L.; Gao, S.; Song, Y.; Che, C. M.; Fun, H. K.; You, X. Z. *Angew. Chem., Int. Ed.* **2000**, *39*, 3633. (b) Mukherjee, P. S.; Maji, T. P.; Escuer, A.; Vicente, R.; Ribas, J.; Rosair, G.; Mautner, F. A.; Chaudhuri, N. R. *Eur. J. Inorg. Chem.* **2002**, 943. (c) Maji, T. K.; Mukherjee, P. S.; Mostafa, G.; Mallah, T.; Cano-Boquera, J.; Chaudhuri, N. R. *Chem. Commun.* **2001**, 1012.
- (13) (a) Munno, G. D.; Lombardi, M. G.; Paoli, P.; Lloret F.; Julve, M. *Inorg. Chim. Acta* **1998**, *282*, 252. (b) Dalai, S.; Mukherjee, P. S.; Drew, M. G. B.; Lu T. H.; Chaudhuri, N. R. *Inorg. Chim. Acta* **2002**, *335*, 85. (c) Goher, M. A. S.; Escuer, A.; Mautner, F. A.; Al-Salem, N. A. *Polyhedron* **2001**, *20*, 2971.
- (14) (a) Shen, Z.; Zuo, J. L.; Yu, Z.; Zhang, Y.; Bai, J. F.; Che, C. M.; Fun, H. K.; Vittal, J. J.; You, X. Z. *Dalton Trans.* **1999**, 3393. (b) Munno, G. D.; Lombardi, M. G.; Julve, M.; Lloret, F.; Faus, J. *Inorg. Chim. Acta* **1998**, *282*, 82 and references therein.
- (15) (a) Maji, T. K.; Mukherjee, P. S.; Koner, S.; Mostafa, G.; Tuchagues, J.-P.; Chaudhuri, N. R. *Inorg. Chim. Acta* **2001**, *314*, 111. (b) Zhang, L.; Tang, L.-F.; Wang, Z.-H.; Du, M.; Julve, M.; Lloret, F.; Wang, J.-T. *Inorg. Chem.* **2001**, *40*, 3619.

- (16) (a) Tandon, S. S.; Thompson, L. K.; Miller, D. O. *J. Chem. Soc., Chem. Commun.* **1995**, 1907. (b) Mautner, F. A.; Hanna, S.; Cortes, R.; Lezama, L.; Gotzone, M.; Rojo, T. *Inorg. Chem.* **1999**, *38*, 4647. (c) Thompson, L. K.; Tandon, S. S.; Lloret, F.; Cano, J.; Julve, M. *Inorg. Chem.* **1997**, *36*, 3301. (d) Chen, H. J.; Mao, Z. W.; Gao, S.; Chen, X. M. *Chem. Commun.* **2001**, 2320.
- (17) Tandon, S. S.; Thompson, L. K.; Manuel, M. E.; Bridson, J. N. *Inorg. Chem.* **1994**, *33*, 5555.
- (18) Mukherjee, P. S.; Maji, T. K.; Mostafa, G.; Mallah, T.; Chaudhuri, N. R. *Inorg. Chem.* **2000**, *39*, 5147.
- (19) House, D. A.; Steel, P. J.; Watson, A. A. *Aust. J. Chem.* **1986**, *39*, 1525.

**Table 1.** Summary of Crystallographic Data for the Complexes

	1	2	3
formula	C <sub>9</sub> H <sub>9</sub> N <sub>9</sub> Cu	C <sub>10</sub> H <sub>11</sub> Cu <sub>2</sub> N <sub>15</sub>	C <sub>9</sub> H <sub>9</sub> MnN <sub>9</sub>
formula weight	306.79	468.42	298.19
crystal system	monoclinic	monoclinic	monoclinic
space group	<i>P</i> 2 <sub>1</sub> / <i>c</i>	<i>P</i> 2 <sub>1</sub> / <i>n</i>	<i>C</i> 2/ <i>c</i>
<i>a</i> , Å	15.4591(3)	11.3117(3)	14.1645(4)
<i>b</i> , Å	10.8105(2)	7.4950(2)	14.5935(4)
<i>c</i> , Å	14.6639(2)	20.9408(7)	12.7881(4)
$\beta$ , deg	101.9938(7)	98.8996(11)	109.5816(14)
<i>U</i> , Å <sup>3</sup>	2397.14(7)	1754.01(9)	2490.54(13)
<i>Z</i>	8	4	8
<i>D</i> <sub>c</sub> , g/cm <sup>3</sup>	1.700	1.774	1.591
$\mu$ (Mo K $\alpha$ ), mm <sup>-1</sup>	1.824	2.457	1.062
<i>T</i> , K	293(2)	293(2)	293(2)
$\theta$ range, deg	3.41–27.48	3.50–27.48	3.50–27.49
reflns measured	47710	26386	22593
unique reflns/ <i>R</i> <sub>int</sub>	5465/0.0818	3998/0.1093	2829/0.0655
params refined	343	232	172
<i>R</i> 1 <sup>a</sup> [ <i>I</i> > 2 $\sigma$ ( <i>I</i> )]	0.0343	0.0620	0.0418
w <i>R</i> 2 <sup>b</sup> (all data)	0.0833	0.1745	0.1180
GOF on <i>F</i> <sup>2</sup>	1.015	1.034	1.026
$\rho_{\max}/\rho_{\min}$ , e Å <sup>-3</sup>	0.913/–0.726	0.786/–0.621	0.655/–0.375

$$^a R1 = \sum ||F_o| - |F_c|| / \sum |F_o|. \quad ^b wR2 = \{ \sum [w(F_o^2 - F_c^2)^2] / \sum [w(F_o^2)^2] \}^{1/2}.$$

mmol) and Cu(ClO<sub>4</sub>)<sub>2</sub>·6H<sub>2</sub>O (0.5 mmol) in 10 mL of methanol. The microcrystalline precipitate formed immediately was collected by filtration, washed with methanol, and dried in air. Yield: 47.7%. The filtrate was left to evaporate slowly at room temperature, yielding dark green crystals within 2 weeks. Yield: 22.8%. Both the precipitate and the crystals exhibit IR spectra identical to that of **1**, and elemental analytical results are also consistent with the composition of **1**. The use of Cu(NO<sub>3</sub>)<sub>2</sub>·6H<sub>2</sub>O, instead of Cu(ClO<sub>4</sub>)<sub>2</sub>·6H<sub>2</sub>O, as the metal source, gave similar results. When an M:L:N<sub>3</sub> ratio of 2:1:4, which corresponds to the stoichiometry of **2**, was used in the above procedure, the precipitate formed immediately was neither **1** nor the compound of formula [Cu<sub>2</sub>(L)(N<sub>3</sub>)<sub>4</sub>]<sub>*n*</sub>, but the crystalline product crystallizing from the filtrate was **1**, according to the IR spectra and analytical data.

[Cu<sub>2</sub>(Me-L)(N<sub>3</sub>)<sub>4</sub>]<sub>*n*</sub> (**2**). This compound was obtained as crystals in a H-shaped tube within 4 weeks, following a procedure similar to that for **1**, with a starting molar ratio of 1:1:2 for M:Me-L:N<sub>3</sub>. Yield: 31.9%. Anal. Calcd for C<sub>10</sub>H<sub>11</sub>Cu<sub>2</sub>N<sub>15</sub>: C 25.64, H 2.37, N 44.86. Found: C 25.86, H 2.64, N 44.85%. Main IR (cm<sup>-1</sup>): 2072vs, 1608m, 1522m, 1448m, 1284m, 765m, 721m. When the reaction ratio was 2:1:4, corresponding to the stoichiometry of **2**, the same compound was obtained with a similar yield. This compound can also be synthesized by mixing the reactants directly, following a procedure similar to that for **1**, with the starting M:Me-L:N<sub>3</sub> ratio being either 1:1:2 or 2:1:4. Both the precipitate formed immediately and the crystals crystallizing from the filtrate are **2**, confirmed by IR spectra and elemental analytical results. Yield: ca. 70%.

[Mn(L)(N<sub>3</sub>)<sub>2</sub>]<sub>*n*</sub> (**3**). A mixture of L (0.50 mmol) and manganese(II) perchlorate hexahydrate (0.50 mmol) in 10 mL of methanol was stirred for 15 min, and then a methanolic solution (10 mL) containing sodium azide (1.0 mmol) was added with continuous stirring. Slow evaporation of the resulting orange solution at room temperature yielded orange crystals of **3** within 2 days. Yield: 32%. Anal. Calcd for C<sub>9</sub>H<sub>9</sub>MnN<sub>9</sub>: C 36.25, H 3.04, N, 42.28. Found: C 35.95, H 3.21, N 42.30. Main IR bands: 2079vs, 2075vs, 1441m, 1405m, 1338m, 1279m, 1064m, 1025m, 760m, 708m.

**Physical Measurements.** Elemental analyses (C, H, N) were performed on an Elementar Varia EL analyzer. IR spectra were recorded on a Nicolet Magna-IR 750 spectrometer equipped with a Nic-Plan Microscope. Variable-temperature magnetic susceptibili-

ties were measured on an Oxford MagLab 2000 magnetometer using samples of ground crystals. Diamagnetic corrections were made with Pascal's constants for all the constituent atoms.<sup>20</sup>

**Crystallographic Studies.** Diffraction intensity data for single crystals of **1–3** were collected at room temperature on a Nonius Kappa CCD area detector equipped with graphite-monochromated Mo K $\alpha$  radiation ( $\lambda = 0.71073$  Å). Empirical absorption corrections were applied using the Sortav program.<sup>21</sup> The structure was solved by the direct method and refined by the full-matrix least-squares method on *F*<sup>2</sup> with anisotropic thermal parameters for all non-hydrogen atoms.<sup>22</sup> Hydrogen atoms were located at calculated positions and refined isotropically using the riding model. Pertinent crystallographic data and structure refinement parameters are summarized in Table 1.

## Results and Discussion

**Syntheses.** The composition and structure of a metal–azido system are obviously sensitive to the coligand used. However, it is difficult to determine a priori, with our present state of knowledge, which bridging mode or polymeric topology will be adopted with a specific coligand.<sup>3</sup> Indeed, for Cu(II) with bidentate coligands, discrete mononuclear and binuclear and polymeric 1D complexes with different bridging networks have been obtained, and no correlation has been found between the properties of the coligand and the structure of the resulting complex.<sup>12–15</sup> In the present case, although the coligands are very similar and the synthetic procedures are essentially identical, compounds **1** and **2** are distinct from each other in stoichiometry and bridging topology. Initially, both compounds were obtained as single crystals by slow diffusion in H-shaped tubes. Mixing the reactants directly in methanol results in microcrystalline precipitates, and slow evaporation of the filtrates yields crystals. When the Me-L ligand was used with the starting metal:ligand:azido ratio being either 1:1:2 or 2:1:4, both the precipitate and the crystals were the 2:1:4 compound, **2**, confirmed by IR spectra and elemental analyses. For the L ligand with a starting ratio of 1:1:2, both products were **1**, of which the composition is consistent with the starting ratio. When a 2:1:4 ratio was used for L, the crystals crystallizing from the filtrate were also **1**, but the precipitate formed immediately was neither **1** nor the 2:1:4 compound. It is likely that the precipitate contains Cu(N<sub>3</sub>)<sub>2</sub>, which precipitated due to the presence of excessive Cu(II) and azido ions in the reaction system.

For Mn(II) with bidentate coligands, we have recently summarized that the resulting complexes generally exhibit 1D chain structures with alternating double EO and double EE bridges. Complex **3**, of formula [Mn(L)(N<sub>3</sub>)<sub>2</sub>]<sub>*n*</sub>, follows this trend. Our attempts to grow suitable crystals of the Mn(II) complex with Me-L were in vain.

The IR spectra of these complexes exhibit characteristic  $\nu_{\text{as}}(\text{N}_3)$  bands in the 2000–2100 cm<sup>-1</sup> region. The occurrence

(20) O'Connor, C. J. *Prog. Inorg. Chem.* **1982**, 29, 203.

(21) (a) Blessing, R. H. *Acta Crystallogr., Sect. A* **1995**, A51, 33. (b) Blessing, R. H. *J. Appl. Crystallogr.* **1997**, 30, 421.

(22) (a) Sheldrick, G. M. *SHELXTL*, Version 5.1; Bruker Analytical X-ray Instruments Inc.: Madison, WI, 1998. (b) Sheldrick, G. M. *SHELXL-97*, PC Version; University of Göttingen: Göttingen, Germany, 1997.

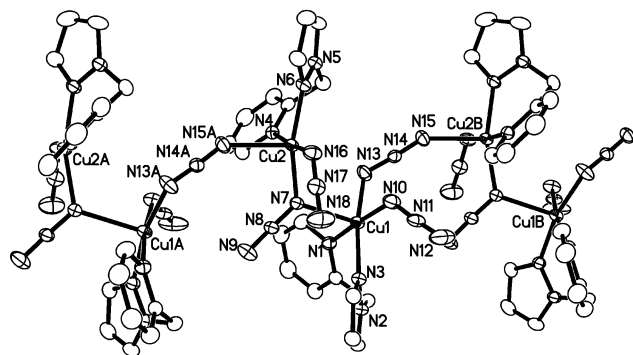


**Figure 1.** Perspective view of the chain structure of **1**.

**Table 2.** Selected Bond Distances (Å) and Angles (deg) for Complex **1**<sup>a</sup>

Cu(1)–N(13)	1.971(2)	Cu(2)–N(16)	1.972(2)
Cu(1)–N(10)	1.979(2)	Cu(2)–N(7)	1.992(2)
Cu(1)–N(3)	2.000(2)	Cu(2)–N(6)	2.013(2)
Cu(1)–N(1)	2.073(2)	Cu(2)–N(4)	2.046(2)
Cu(1)–N(7)	2.341(2)	Cu(2)–N(15A)	2.355(2)
N(7)–N(8)	1.189(3)	N(10)–N(11)	1.171(3)
N(8)–N(9)	1.141(3)	N(11)–N(12)	1.147(4)
N(13)–N(14)	1.187(3)	N(16)–N(17)	1.186(3)
N(14)–N(15)	1.149(3)	N(17)–N(18)	1.148(3)
N(13)–Cu(1)–N(10)	89.38(10)	N(16)–Cu(2)–N(7)	94.40(9)
N(13)–Cu(1)–N(3)	167.52(10)	N(16)–Cu(2)–N(6)	87.99(9)
N(10)–Cu(1)–N(3)	93.32(10)	N(7)–Cu(2)–N(6)	162.36(9)
N(13)–Cu(1)–N(1)	87.92(10)	N(16)–Cu(2)–N(4)	174.99(9)
N(10)–Cu(1)–N(1)	173.34(10)	N(7)–Cu(2)–N(4)	90.50(9)
N(3)–Cu(1)–N(1)	88.05(9)	N(6)–Cu(2)–N(4)	87.02(9)
N(13)–Cu(1)–N(7)	94.36(9)	N(16)–Cu(2)–N(15A)	91.39(9)
N(10)–Cu(1)–N(7)	94.56(9)	N(7)–Cu(2)–N(15A)	99.08(8)
N(3)–Cu(1)–N(7)	97.56(8)	N(6)–Cu(2)–N(15A)	98.34(9)
N(1)–Cu(1)–N(7)	91.72(8)	N(4)–Cu(2)–N(15A)	88.85(8)
Cu(2)–N(7)–Cu(1)	116.60(9)	N(14)–N(13)–Cu(1)	120.47(19)
N(8)–N(7)–Cu(2)	122.28(18)	N(14)–N(15)–Cu(2B)	143.4(2)
N(8)–N(7)–Cu(1)	120.66(17)	N(15)–N(14)–N(13)	177.7(3)
N(9)–N(8)–N(7)	176.0(3)	N(12)–N(11)–N(10)	175.7(3)

<sup>a</sup> Symmetry transformations: A,  $x, -y + 1/2, z - 1/2$ ; B,  $x, -y + 1/2, z + 1/2$ .

of two sharp and strong bands, observed at 2064 and 2038  $\text{cm}^{-1}$  for **1**, and 2079 and 2075  $\text{cm}^{-1}$  for **3**, indicates the presence of two different azido groups. The band of higher frequency is attributable to the EO bridge, and the other is attributable to the EE bridge.<sup>7a,17</sup> For **2**, only a very strong absorption band around 2072  $\text{cm}^{-1}$  is found in the region, but it is broader than those for **1** and **3**, attributable to the envelope of the  $\nu_{\text{as}}(\text{N}_3)$  absorptions of the three different types of EO azido bridges.

**Structures of the Cu(II) Complexes.** The structure of **1** consists of 1D zigzag Cu(II)–azido chains, in which the Cu(II) ions are alternately linked by single EO and single EE azido bridges (Figure 1). Selected bond parameters are collected in Table 2.

There are two crystallographically independent sets of Cu(II) ions and three types of azido ligands in different coordination modes. Each Cu(II) ion is ligated by a bidentate L ligand, a terminal azido ion, a EO azido bridge, and a EE azido bridge, with a distorted square pyramidal geometry. The Cu–N(pyridyl) distances (average 2.06 Å) are longer than the Cu–N(pyrazole) ones (average 2.006 Å), which is in agreement with the trend observed for  $[\text{Co}(\text{L})_2\text{Cl}_2] \cdot 4\text{H}_2\text{O}$ <sup>23a</sup>

and  $[\text{Cu}(\text{Me}_2\text{-L})_2](\text{ClO}_4)_2 \cdot \text{H}_2\text{O}$ ,<sup>23b</sup> but opposite that for  $[\text{Cu}(\text{Me}_2\text{-L})_2(\text{NO}_2)](\text{ClO}_4)$  [ $\text{Me}_2\text{-L} = 2\text{-}(3,5\text{-dimethylpyrazol-1-ylmethyl})\text{pyridine}$ ].<sup>23c</sup> The apical position of Cu1 is occupied by the EO azido ion and that of Cu2 by the EE ion, with the apical Cu–N distances significantly longer than the basal ones. The average deviations of the basal donors from the mean basal plane are 0.048 Å for Cu1 and 0.150 Å for Cu2, and the Cu atoms are displaced out of the basal planes by 0.160(1) and 0.155(1) Å for Cu1 and Cu2, respectively, toward the apical donors. The geometry around Cu1 is less distorted than that around Cu2. According to Addison et al.,<sup>24</sup> the distortion of the square pyramidal geometry toward trigonal bipyramidal can be described by the geometrical parameter  $\tau = |\beta - \alpha|/60$ , where  $\beta$  and  $\alpha$  are the bond angles involving the trans donor atoms in the basal plane. The  $\tau$  values are 0.097 and 0.21 for Cu1 and Cu2, respectively. All azido ions are quasi-linear and exhibit asymmetric N–N distances. The Cu–N<sub>3</sub>–Cu torsion angle and the Cu $\cdots$ Cu distance in the EE bridging moiety are 69.8(2)° and 5.590 Å, respectively, while the Cu $\cdots$ Cu distance spanned by the EO bridge is 3.691 Å. It is interesting to note that both EO and EE bridges assume an asymmetric apical–basal disposition between neighboring Cu(II) ions; i.e., the same azido bridge resides on the apical position of one copper but in the basal plane of the neighboring copper, with the apical Cu–N distance being significantly longer than the basal one. In the lattice, the chains run along the  $c$  direction and there is no evident indication of interchain  $\pi$ – $\pi$  interactions. The shortest Cu $\cdots$ Cu interchain distance is 8.128 Å between Cu1 and Cu2 ( $2 - x, y - 0.5, 0.5 - z$ ).

Compound **2**, with a different formula,  $[\text{Cu}_2(\text{Me-L})(\text{N}_3)_4]_n$ , also consists of 1D Cu(II)–azido chains, but the chain topology is completely different (Figure 2). Selected bond parameters are collected in Table 3. There are two nonequivalent Cu(II) ions, each assuming the distorted square pyramidal geometry, and four nonequivalent azido ligands, all of which adopt the EO bridging mode. Two nitrogen atoms from Me-L and three nitrogen atoms from azido ions define the geometry around Cu1, with an azido nitrogen atom (N13) on the apical position. The Cu–N(Me-L) distances are shorter than those in **1**, with the Cu–N(pyridyl) distance (2.009 Å) slightly longer than the Cu–N(pyrazole) one (1.979 Å). For the Cu2 atom, only azido ions are involved in the coordination, with N10B on the apical position. The largest deviations of the basal donors from the mean basal plane are 0.178 Å for Cu1 and 0.303 Å for Cu2, and the Cu atoms are 0.237 and 0.132 Å out of the basal planes for Cu1 and Cu2, respectively. The distortion parameters of the square pyramidal geometry are  $\tau = 0.27$  and 0.21 for Cu1 and Cu2, respectively. All azido ions are quasi-linear, and exhibit asymmetric N–N distances, as observed in **2**. Four Cu(II) ions and six azido bridges form a unique centrosymmetric tetranuclear ring, within which the Cu(II) ions are alternately

(23) (a) Lal, T. K.; Mukherjee, R. *Polyhedron* **1997**, *16*, 3577. (b) Gupta, R.; Lal, T. K.; Mukherjee, R. *Polyhedron* **2002**, *21*, 1245. (c) Lal, T. K.; Richardson, J. F.; Mashuta, M. S.; Buchanan, R. M.; Mukherjee, R. *Polyhedron* **1997**, *16*, 4331.

(24) Addison, W.; Rao, T. N.; Reedijk, J.; van Rijn, J.; Verschoor, G. C. *Dalton Trans.* **1984**, 1349.

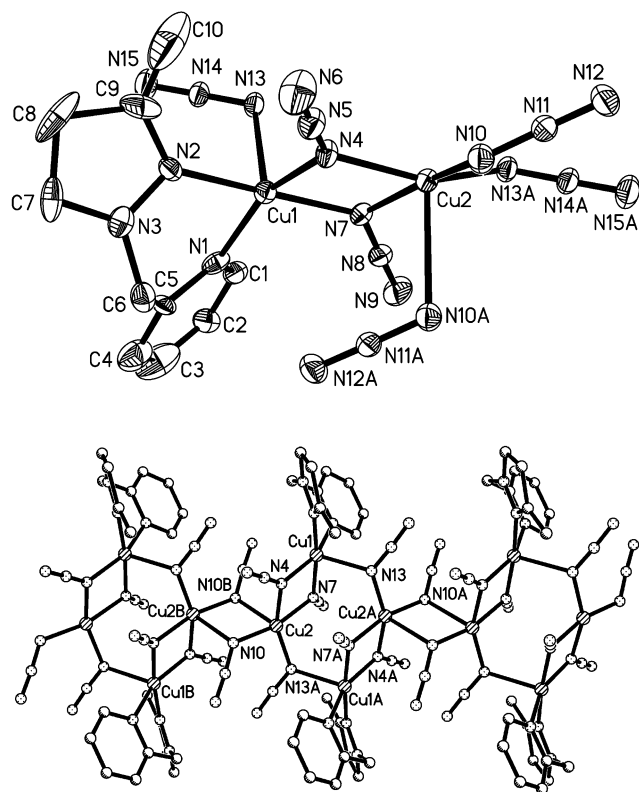


**Figure 2.** Perspective views showing the atomic labeling scheme and metal coordination environments (top) and the chain topology (bottom) in **2**.

**Table 3.** Selected Bond Distances (Å) and Angles (deg) for Complex **2**<sup>a</sup>

Cu(1)–N(2)	1.979(5)	Cu(2)–N(10)	1.958(6)
Cu(1)–N(4)	1.982(5)	Cu(2)–N(13)#1	1.970(5)
Cu(1)–N(1)	2.009(3)	Cu(2)–N(4)	2.002(5)
Cu(1)–N(7)	2.011(5)	Cu(2)–N(7)	2.040(5)
Cu(1)–N(13)	2.297(5)	Cu(2)–N(10B)	2.566(6)
N(4)–N(5)	1.185(8)	N(10)–N(11)	1.203(8)
N(5)–N(6)	1.119(8)	N(11)–N(12)	1.131(8)
N(7)–N(8)	1.214(7)	N(13)–N(14)	1.189(7)
N(8)–N(9)	1.128(7)	N(14)–N(15)	1.131(8)
N(2)–Cu(1)–N(4)	94.7(2)	N(10)–Cu(2)–N(13A)	98.4(3)
N(2)–Cu(1)–N(1)	87.9(2)	N(10)–Cu(2)–N(4)	93.6(2)
N(4)–Cu(1)–N(1)	156.3(2)	N(13A)–Cu(2)–N(4)	154.0(2)
N(2)–Cu(1)–N(7)	172.9(2)	N(10)–Cu(2)–N(7)	166.3(2)
N(4)–Cu(1)–N(7)	78.7(2)	N(13A)–Cu(2)–N(7)	93.9(2)
N(1)–Cu(1)–N(7)	97.06(19)	N(4)–Cu(2)–N(7)	77.6(2)
N(2)–Cu(1)–N(13)	92.2(2)	N(10)–Cu(2)–N(10B)	85.1(2)
N(4)–Cu(1)–N(13)	106.5(2)	N(13A)–Cu(2)–N(10B)	106.6(2)
N(1)–Cu(1)–N(13)	96.94(19)	N(4)–Cu(2)–N(10B)	97.3(2)
N(7)–Cu(1)–N(13)	92.28(19)	N(7)–Cu(2)–N(10B)	85.68(19)
Cu(1)–N(4)–Cu(2)	103.0(2)	Cu(2)–N(10)–Cu(2B)	94.9(2)
N(6)–N(5)–N(4)	178.6(8)	N(12)–N(11)–N(10)	176.2(8)
Cu(1)–N(7)–Cu(2)	100.7(2)	Cu(2A)–N(13)–Cu(1)	110.9(2)
N(9)–N(8)–N(7)	178.9(8)	N(15)–N(14)–N(13)	176.0(8)

<sup>a</sup> Symmetry transformations: A,  $-x + 2, -y + 1, -z$ ; B,  $-x + 2, -y + 2, -z$ .

bridged by single azido (N13–N14–N15) and double azido (N4–N5–N6 and N7–N8–N9) bridges. The azido ions in the doubly bridging moiety take a quasi-symmetric basal–basal disposition by occupying the basal positions of both Cu1 and Cu2 with the Cu–N distances in the 1.98–2.04 Å range. However, the single azido bridge is disposed in an asymmetric apical–basal fashion, as observed in **1**. The coordination of Cu2 is completed by two extraannular azido

ions, which serve as a double bridge between two Cu2 atoms of different rings. In such a way, adjacent tetranuclear rings are interlinked into an exotic “chain of rings”. The interannular bridges are highly asymmetric with an apical–basal disposition, the apical Cu–N distance being significantly longer than the basal one. The Cu···Cu distances spanned by different azido bridges are 3.118(1), 3.359(2), and 3.520(1) Å, for the intraannular double bridge, the interannular double bridge, and the intraannular single bridge, respectively. The chains in **2** are packed in parallel along the *b* direction. The shortest Cu···Cu interchain distance is 8.486 Å between Cu1 and Cu1 ( $3/2 - x, y - 1/2, 1/2 - z$ ). There are no evident indications of interchain hydrogen bonding or  $\pi$ – $\pi$  interactions.

The most interesting structural feature of **2** is the exotic and unprecedented “chain of rings” topology built via three different kinds of EO azido bridges. On the other hand, the occurrence of the EO bridge as the only linkage between two metal ions in **1** and **2** is also unusual, since the EO bridge tends to coexist with other bridging groups.

**Structure of the Mn(II) Complex.** The structure of **3** consists of 1D Mn(II)–azido chains. A perspective view of the chain structure is depicted in Figure 3, and selected bond lengths and angles are listed in Table 4. The adjacent Mn(II) ions in a chain are linked alternately by double end-on and double end-to-end azido bridges with the Mn–N(azido) distances in the 2.218(3)–2.303(2) Å range. The EO azido bridges show slightly asymmetric N–N distances, but the EE bridges are essentially symmetric. These are consistent with similar Mn–azido chain compounds with alternating double EO and double EE azido bridges.<sup>6</sup> The cis-octahedral coordination polyhedron around Mn(II) is completed by the two nitrogen atoms (N1 and N3) from the L ligand with longer Mn–N distances. The neighboring Mn(II) ions bridged by double EO azido ions are interrelated by a 2-fold axis. The resulting Mn1–N7–Mn1B–N7A ring is quasi-planar with all of the atoms deviating from their mean plane by only 0.016 Å. The Mn···Mn distance is 3.461 Å, and the Mn1–N7–Mn1B angle is 101.96(9)°, which lies within the range for Mn(II) ions with EO azido bridges (99.6–105°).<sup>6</sup> The neighboring Mn(II) ions bridged by double EE azido ions are interrelated by an inversion center. The Mn–azido–Mn torsion angle  $\tau$ , defined by the dihedral angle between the mean planes of Mn1–N4–N5–N6 and Mn1A–N6–N5–N4, is 37.8(2)°. The two EE azido bridges are parallel and thus form a plane, which is characteristic of most polynuclear complexes with double EE azido bridges.<sup>3,6</sup> The Mn(II) ions are 0.529(5) Å out of the (EE–N<sub>3</sub>)<sub>2</sub> plane, and the dihedral angle  $\delta$  between this plane and the N6–Mn1–N8B plane is only 19.59(8)°, indicating a slight chair conformation for the Mn–(N<sub>3</sub>)<sub>2</sub>–Mn ring. The Mn···Mn distance spanned by the EE bridge is 5.405 Å. The structural parameters for the EE bridging moiety are comparable to those for the compounds reported elsewhere.<sup>6</sup> The  $\tau$  and  $\delta$  angles are very similar to those ( $\tau = 37.2^\circ$  and  $\delta = 19.6^\circ$ ) of [Mn(L')(N<sub>3</sub>)<sub>2</sub>]<sub>n</sub> (L' is the bidentate Schiff base obtained from the condensation of 2-pyridylaldehyde with *m*-toluidine).<sup>6</sup>

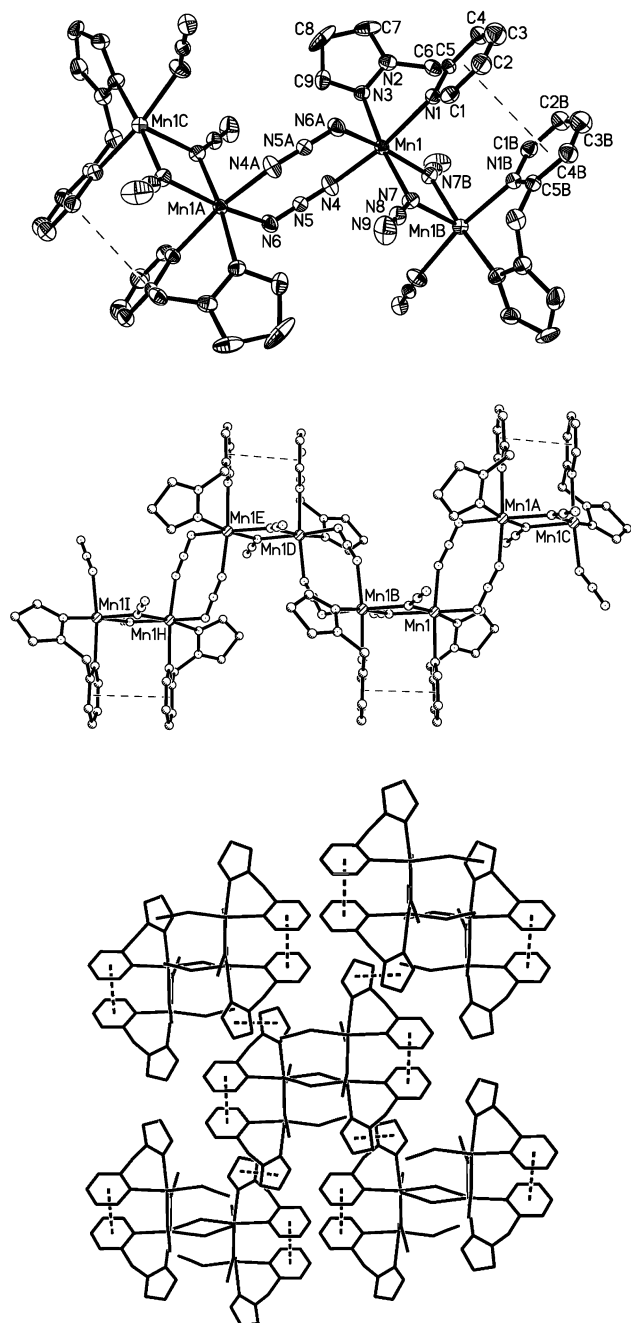


**Figure 3.** Perspective views showing the metal coordination environments (top), the chain topology with intrachain  $\pi$ - $\pi$  interactions (middle), and the intra- and interchain  $\pi$ - $\pi$  interactions (bottom) in **3**.

Although the bridging mode of the azido ion in **3** is similar to those in other Mn(II) chains with alternate double EO and EE bridges, the overall shape of the present chain is unique in that it assumes a concavo-convex arrangement, as shown in Figure 3 (bottom). The difference is phenomenologically due to the presence of the 2-fold axis instead of an inversion center between the EO azido-bridged Mn(II) ions. It is interesting to note that the chain structure may be further stabilized by intrachain  $\pi$ - $\pi$  interactions. The two pyridyl rings bound to the two EO-bridged adjacent Mn(II) ions are quasi-parallel with a dihedral angle of  $2.2^\circ$ , and the centroid-centroid distance of the two pyridyl rings is  $3.583 \text{ \AA}$  with nearly half the rings overlapping. This clearly

**Table 4.** Selected Bond Distances ( $\text{\AA}$ ) and Angles (deg) for Complexes **3**<sup>a</sup>

Mn(1)-N(4)	2.218(3)	Mn(1)-N(1)	2.303(2)
Mn(1)-N(6A)	2.240(3)	N(4)-N(5)	1.166(3)
Mn(1)-N(7)	2.230(2)	N(5)-N(6)	1.169(3)
Mn(1)-N(7B)	2.225(2)	N(7)-N(8)	1.182(3)
Mn(1)-N(3)	2.270(2)	N(8)-N(9)	1.153(4)
N(4)-Mn(1)-N(7B)	92.52(9)	N(7B)-Mn(1)-N(1)	89.64(8)
N(4)-Mn(1)-N(7)	96.73(10)	N(7)-Mn(1)-N(1)	93.30(8)
N(7B)-Mn(1)-N(7)	78.02(9)	N(6A)-Mn(1)-N(1)	90.07(9)
N(4)-Mn(1)-N(6A)	89.88(10)	N(3)-Mn(1)-N(1)	80.56(8)
N(7B)-Mn(1)-N(6A)	167.78(9)	Mn(1B)-N(7)-Mn(1)	101.96(9)
N(7)-Mn(1)-N(6A)	89.80(9)	N(5)-N(4)-Mn(1)	135.6(2)
N(4)-Mn(1)-N(3)	89.42(10)	N(5)-N(6)-Mn(1A)	125.0(2)
N(7B)-Mn(1)-N(3)	99.09(9)	N(8)-N(7)-Mn(1B)	129.1(2)
N(7)-Mn(1)-N(3)	173.28(9)	N(8)-N(7)-Mn(1)	128.2(2)
N(6A)-Mn(1)-N(3)	92.92(10)	N(4)-N(5)-N(6)	176.7(3)
N(4)-Mn(1)-N(1)	169.97(10)	N(9)-N(8)-N(7)	178.5(3)

<sup>a</sup> Symmetry codes: A,  $-x, -y, -z$ ; B,  $-x, y, -z + 1/2$ .

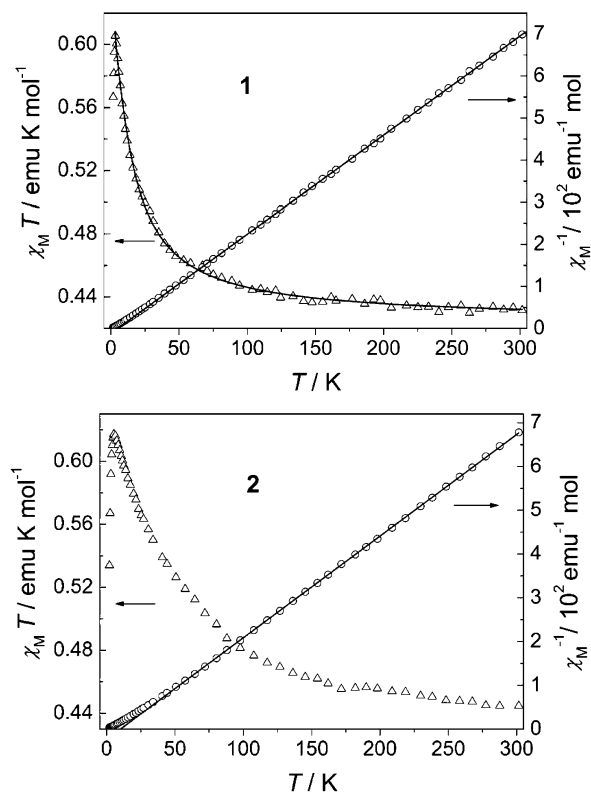


**Figure 4.** Temperature dependence of magnetic susceptibility for **1** and **2**.

indicates the presence of  $\pi$ - $\pi$  interactions within the chain. The chains run along the  $c$  direction and are stacked in parallel in the lattice, and the shortest interchain Mn $\cdots$ Mn distance is  $8.339 \text{ \AA}$ . Further investigation reveals there is a weak interchain  $\pi$ - $\pi$  interaction between two pyrazole rings related by an inversion center ( $1/2 - x, 1/2 - y, -z$ ): the conjugated C=C=C=N parts of the two parallel pyrazole rings overlap with each other, and the centroid-centroid distance is  $3.895 \text{ \AA}$ . Thus, each chain interacts with four neighbors to generate a supramolecular three-dimensional structure (Figure 4).

**Magnetic Properties of the Cu(II) Complexes.** The magnetic susceptibilities of the complexes were measured in the 2–300 K temperature range and are shown as  $\chi_M T$  and  $\chi_M^{-1}$  versus  $T$  plots in Figure 4. The  $\chi_M T$  values per

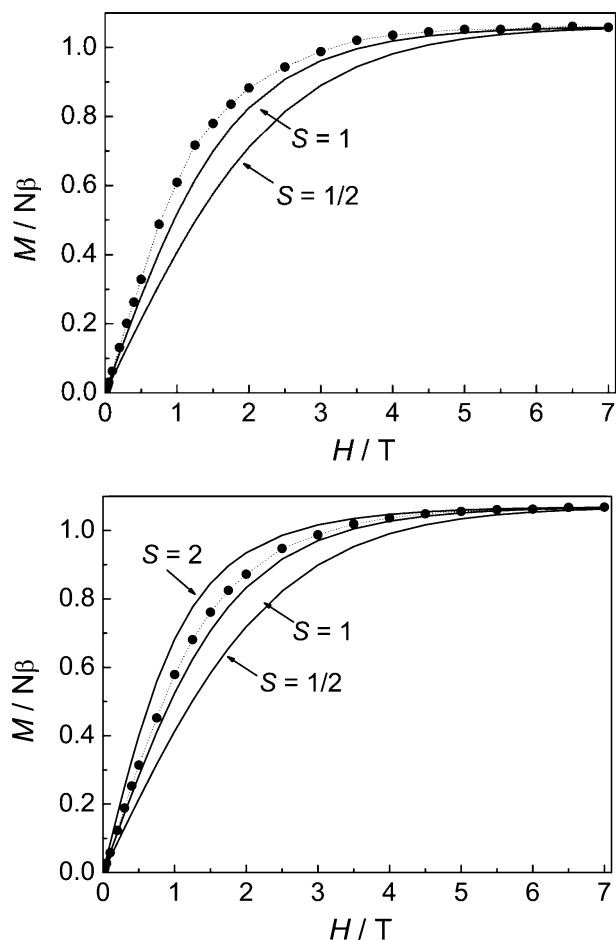


**Figure 5.** Field-dependent magnetization of complexes **1** (top) and **2** (bottom).

Cu(II) ion at 300 K are 0.43 and 0.44  $\text{emu mol}^{-1} \text{K}$  for **1** and **2**, respectively. Upon cooling to 2 K, the  $\chi_M$  values increase monotonically but the  $\chi_M T$  products increase to a maximum at 3 K for **1** and 5 K for **2**, suggesting overall ferromagnetic interactions for both complexes. The low-temperature drops in  $\chi_M T$  may be due to secondary antiferromagnetic interactions and/or zero-field splitting effects. The secondary antiferromagnetic interactions may be intra- or interchain (vide infra). The high-temperature linear parts of the  $1/\chi_M$  vs  $T$  plots obey the Curie–Weiss law, the fit constants being  $C = 0.42 \text{ emu mol}^{-1} \text{K}$  with  $\theta = 4.9 \text{ K}$  for **1**, and  $C = 0.43 \text{ emu mol}^{-1} \text{K}$  with  $\theta = 10.2 \text{ K}$  for **2**. The positive Weiss constants support the overall ferromagnetic interactions, and the Curie values correspond to the values expected for Cu(II) ions with  $g = 2.12$  and  $2.14$  for **1** and **2**, respectively.

Further support for the ferromagnetic interactions comes from field-dependent magnetization measured at 1.8 K (Figure 5). As the field is increased, the magnetization saturates rapidly and reaches  $1.06 N\beta$  for **1** and  $1.07 N\beta$  for **2**. The saturation values are in good agreement with the  $g$  factors estimated from the Curie–Weiss law. The experimental  $M$ – $H$  curves are above those predicted by the Brillouin function for an isolated Cu(II) ion using the above  $g$  values (Figure 5,  $S = 1/2$ ), clearly suggesting the presence of ferromagnetic interactions.

The structure of **1** suggests two alternating magnetic interactions along the chain through the single EO and EE azido bridges, respectively. To achieve an overall ferromagnetic effect, the coupling scheme may be a dominant F interaction alternating with a weaker AF interaction, a ferromagnetic interaction alternating with a negligible interaction, or two F interactions alternating. Although the first scheme seems to be consistent with the low-temperature drop in  $\chi_M T$ , it should be ruled out because the  $\chi_M T$  maximum [ $0.61 \text{ emu mol}^{-1} \text{K}$  per Cu(II)] is higher than the maximum [ $0.56 \text{ emu mol}^{-1} \text{K}$  per Cu(II)] that can be reached by two ferromagnetically coupled Cu(II) ions ( $S = 1$ ) with  $g = 2.12$ . The second scheme is ruled out for the same reason. Therefore, the third coupling scheme with two alternating F interactions should be the only choice. This is also supported by the field dependence of magnetization: the magnetization of **1** saturates more rapidly than predicted by the Brillouin function for the triplet state of a ferromagnetic binuclear Cu(II) molecule ( $S = 1$ , Figure 5, top), indicating an additional F interaction between the imaginary binuclear molecules. Since both intrachain interactions are ferromagnetic, the low-temperature drop in  $\chi_M T$  may arise from interchain antiferromagnetic interactions and/or the zero-field splitting effects of the high-spin ground state. With no analytical expression of magnetic susceptibility having yet been proposed for alternating ferromagnetic chains with  $S = 1/2$  local spins, we applied an approximate approach to evaluate the interactions. In the approach, the chain is treated as a chain of  $\text{Cu}_2$  dimers. The “intradimer” interaction ( $J$ ) is expressed in the well-known Bleaney–Bowers equation,<sup>25</sup> and then the other interaction is treated as the “interdimer” interaction ( $zJ'$ ) using the molecular-field approximation:<sup>20</sup>

$$\chi = \chi_{\text{dimer}} / [1 - (zJ'/Ng^2\beta^2)\chi_{\text{dimer}}] \quad (1)$$

The fit of the experimental data of **1** above 3 K by the above approach led to  $g = 2.13(1)$ ,  $J = 14.1(2) \text{ cm}^{-1}$  and  $zJ' = 0.45(1) \text{ cm}^{-1}$  (all  $J$ 's are based on  $\mathbf{H} = -J\mathbf{S}_1 \cdot \mathbf{S}_2$ ). Since the EE bridging moiety has three atoms between metal ions and the  $\text{Cu} \cdots \text{Cu}$  distance is much longer than that for the EO bridge, we tentatively assign  $J$  and  $zJ'$  to the EO and EE bridges, respectively.

It is interesting to note that **4**, the only compound that was previously shown to contain single EO and single EE bridges, exhibits alternating AF/AF interactions,<sup>18</sup> just opposite those in **1**. For the single EO bridge, the Cu–N–Cu angles is  $116.6^\circ$  in **1** and  $130^\circ$  in **4**.<sup>21</sup> It is likely that the much smaller bridging angle in **1** helps to arrange the magnetic orbitals in appropriate orientations so that an accident orthogonality is achieved. It has been widely cited that the interaction through an EO azido bridge is ferromagnetic for lower Cu–N–Cu angles and antiferromagnetic for higher angles. The critical angle is  $104^\circ$  according to empirical analyses<sup>17</sup> and  $108^\circ$  according to a density functional study.<sup>26</sup> It appears that the ferromagnetic interaction in **1**, with a Cu–N–Cu angle of  $116.6^\circ$ , disagrees with the above trends.

(25) Bleaney, B.; Bowers, K. D. *Proc. R. Soc. London, Ser. A* **1952**, *214*, 451.

**Table 5.** Structural and Magnetic Parameters for Asymmetric EO Bridges

complex <sup>a</sup>	Cu–N <sup>b</sup> (Å)	α <sup>c</sup> (deg)	d <sup>d</sup> (Å)	τ <sup>e</sup>	J (cm <sup>-1</sup> )	ref
Single EO						
[Cu(hppz)(N <sub>3</sub> ) <sub>2</sub> ] <sub>n</sub> <sup>a</sup>	2.28	123.0	3.88	0.02, 0.10	–11.5	18
<b>6</b> <sup>a</sup>	2.34	116.6	3.69	0.21, 0.10	14.1	this work
<b>7</b> <sup>b</sup>	2.30	110.9	3.52	0.21, 0.28		this work
Double EO						
<b>7</b>	2.57	94.9	3.36	0.28		this work
[Cu(dpt)(N <sub>3</sub> ) <sub>2</sub> (ClO <sub>4</sub> ) <sub>2</sub> ]	2.35	100.9	3.36	0.28, 0.49	–1	27a
[Cu(terpy)(H <sub>2</sub> O)(N <sub>3</sub> ) <sub>2</sub> (PF <sub>6</sub> ) <sub>2</sub> ]	2.85	95.7	3.60	0.06	–2.9	27b
[Cu(bipy)(N <sub>3</sub> ) <sub>2</sub> ] <sub>n</sub>	2.68	96.8	3.51	0.06	–2.7	14b
[Cu(bipy)(N <sub>3</sub> ) <sub>2</sub> ] <sub>n</sub>	2.60	96.2	3.43	0.01	4.6	14b
Cu(dmbpy)(N <sub>3</sub> ) <sub>2</sub> <sub>n</sub>	2.63	97.0	3.49	0.001	7.6	14a
[Cu <sub>2</sub> (L <sup>1</sup> ) <sub>2</sub> (N <sub>3</sub> ) <sub>2</sub> ]	2.55	86.9	3.17	0.18	24	27c

<sup>a</sup> hppz = homopiperazine; dpt = dipropylenetriamine; terpy = 2,2':6'2''-terpyridine; bipy = 2,2'-bipyridine; dmbpy = 4,4'-dimethyl-2,2'-bipyridine; L<sup>1</sup> = 7-amino-4-methyl-5-aza-3-hepten-2-onato. <sup>b</sup> The apical Cu–N(azido) bond distances. <sup>c</sup> The Cu–N–Cu bridging angle. <sup>d</sup> The Cu···Cu distance spanned by the EO bridge. <sup>e</sup> The distortion parameter of the coordination geometry around the Cu atom.<sup>24</sup>

**Table 6.** Structural and Magnetic Parameters for Single Asymmetric EE Bridges

complex <sup>a</sup>	Cu–N <sup>b</sup> (Å)	θ <sup>c</sup> (deg)	Cu–N–N (deg)	d <sup>d</sup> (Å)	τ <sup>e</sup>	J (cm <sup>-1</sup> )	ref
<b>6</b> <sup>a</sup>	2.36	69.8	120.5, 143.4	5.59	0.21, 0.097	0.45	this work
[Cu(bzam)(N <sub>3</sub> ) <sub>2</sub> ] <sub>n</sub>	2.33	102.1	121.5, 144.6	5.75	0.01	0.58	12a
[Cu(hppz)(N <sub>3</sub> ) <sub>2</sub> ] <sub>n</sub>	2.30	55.3	122.2, 151.4	5.63	0.022, 0.10	–2.7	18
[Cu(bpym)(N <sub>3</sub> ) <sub>2</sub> ] <sub>n</sub>	2.47	f	108.2, 124.1	5.06	0.07	–3.8	13a
[Cu(py) <sub>3</sub> (N <sub>3</sub> )](PF <sub>6</sub> )	2.36	124.1	123.6, 161.3	6.12	0.18	1.84	13c
[Cu(L1)(N <sub>3</sub> ) <sub>2</sub> ] <sub>n</sub>	2.36	97.8	126.5, 131.2	5.69	0.083	2.15	12b
[Cu(L2)(N <sub>3</sub> ) <sub>2</sub> ] <sub>n</sub>	2.31	50.0	131.2, 139.1	5.63	0.17	3.61	12b
[Cu(L3)(N <sub>3</sub> ) <sub>2</sub> ] <sub>n</sub>	2.27	40.4	139.0, 132.2	5.54	0.15	2.06	12b
[Cu(L4)(N <sub>3</sub> ) <sub>2</sub> ] <sub>n</sub>	2.27	31.4	134.4, 136.7	5.59	0.12	2.69	13b
[Cu(L5)(N <sub>3</sub> ) <sub>2</sub> ] <sub>n</sub>	2.40	102.8	122.5, 135.1	5.74	0.13	2.02	13b
[Cu(L6)(N <sub>3</sub> ) <sub>2</sub> ] <sub>n</sub>	2.49	88.4	125.6, 135.7	5.77	0.15	1.36	12c

<sup>a</sup> bzam = benzylamine; hppz = homopiperazine; bpym = 2,2'-bipyrimidine. Li (*i* = 1–6) are the Schiff bases obtained from the condensation of pyridine-2-carbaldehyde with *N,N*-dimethylethane-1,2-diamine (L1), *N,N*-diethylethane-1,2-diamine (L2), 4-(2-aminoethyl)morpholine (L3), *N,N*,2,2-tetramethylpropane-1,3-diamine (L4), 1-(dimethylamino)-2-propylamine (L5), and 1-(2-aminoethyl)piperidine (L6), respectively. <sup>b</sup> The apical Cu–N(azido) bond distances. <sup>c</sup> The Cu–N<sub>3</sub>–Cu torsion angle. <sup>d</sup> The Cu···Cu distance spanned by the EE bridge. <sup>e</sup> The distortion parameter of the coordination geometry around the Cu atom.<sup>24</sup> <sup>f</sup> Not available.

However, the trends are based on basal–basal EO azido bridges that exist in pairs or coexist with other bridging groups, so it is not a surprise that the asymmetric azido bridge disposed in a basal–apical fashion does not follow the trends. Theoretical studies have not been reported for this type of bridges. This type of EO azido bridge has also been found to exist in pairs, forming a double asymmetric bridge. We have collected the structural and magnetic data for both single and double asymmetric EO azido bridges in the literature for the purpose of magnetostructural correlations. Unfortunately, the data are limited and so dispersed that no meaningful statements can be made (Table 5).

Cu(II) species with single EE bridges are more common than those with single EO bridges. A collection of the structural and magnetic data in the literature is given in Table 6. Both F and AF interactions have been reported for this type of bridges. Some tentative correlations have been proposed between the magnetic parameter (*J*) and some structural parameters, such as the Cu–N<sub>3</sub>–Cu torsion angle<sup>12</sup> or the distortion of the Cu(II) coordination geometry,<sup>13</sup> but they were restricted to a limited number of data and are not applicable in a general sense. More experimental data and theoretical studies are needed to establish a meaningful and general magnetostructural correlation.

According to the structural and magnetic data of **2**, three different interactions with global F interactions are operative

through the three different kinds of EO azido bridges. As analyzed for **1**, the  $\chi_{MT}$  maximum [0.62 emu mol<sup>-1</sup> K per Cu(II)] and the field-dependent magnetization for **2** are above the corresponding values expected for two ferromagnetically coupled Cu(II) ions (*S* = 1, Figure 5, bottom), suggesting the presence of two F interactions. Furthermore, the field-dependent magnetization is somewhat lower than that expected for four ferromagnetically coupled Cu(II) ions (*S* = 2, Figure 5, bottom), perhaps indicating that the third interaction is antiferromagnetic. This intrachain interaction should, at least partially, be responsible for the low-temperature drop in  $\chi_{MT}$  of **2**. However, the contributions from interchain antiferromagnetic interactions and the zero-field splitting effects cannot be ruled out.

The lack of an appropriate magnetic model to describe the complicated situation in **2** precludes quantitative magnetic analyses. However, we believe that the interaction through the intraannular double bridges, which assume the basal–basal disposition with Cu–N–Cu angles of 103.0(2)° and 100.7(2)°, is ferromagnetic and stronger than those through the other bridges, since the basal–basal disposition ensures an effective delocalization of the magnetic orbitals toward the bridging atom and the Cu–N–Cu angles lie within the range for ferromagnetic interactions.<sup>17,26</sup> In fact, the double EO bridge with symmetric or pseudosymmetric basal–basal disposition has always been found to mediate medium or strong ferromagnetic exchange between Cu(II) ions (23–

(26) Ruiz, E.; Cano, J.; Alvarez, S.; Alemany, P. *J. Am. Chem. Soc.* **1998**, *120*, 11122.



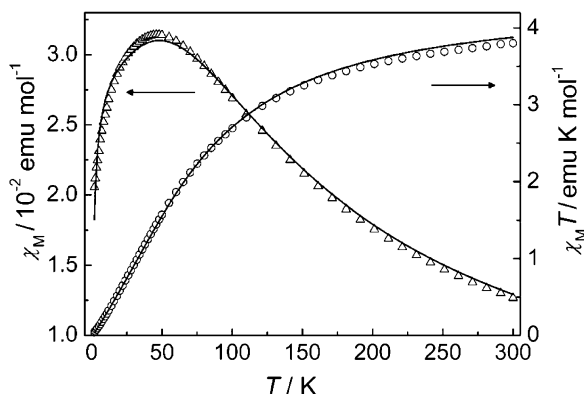


**Figure 6.** Temperature dependence of magnetic susceptibility for **3**. The solid lines represent the best fit of the experimental data.

105  $\text{cm}^{-1}$ ).<sup>28</sup> For the asymmetric apical–basal double or single EO bridges, both F and AF interactions have been reported, and magnetostructural correlations remain unclear with limited data (Table 5). Thus, it is difficult to determine the signs of the interactions through the asymmetric bridges.

**Magnetic Properties of the Mn(II) Complex.** The magnetic susceptibility of complex **3** was measured in the 2–300 K temperature range and is shown as  $\chi_M$  and  $\chi_M T$  versus  $T$  plots in Figure 6. The experimental  $\chi_M T$  value at 300 K is 3.80  $\text{emu mol}^{-1} \text{K}$ , somewhat lower than the spin-only value (4.38  $\text{emu K mol}^{-1}$ ) expected for an uncoupled high-spin Mn(II) ion. Upon cooling, the  $\chi_M T$  product decreases monotonically and tends to zero at low temperature, while the  $\chi_M$  value increases to a rounded maximum at about 47 K and then decreases rapidly on further cooling. These features indicate a dominant antiferromagnetic interaction in the compound.

According to the structural data, compound **3** should exhibit alternating ferro- and antiferromagnetic interactions mediated by double EO and double EE azido bridges, respectively.<sup>6,7</sup> To simulate the experimental magnetic behavior, we used the theoretical model proposed by Cortés et al. for alternating F/AF  $S = 5/2$  chains.<sup>7a</sup> The expression of the molar susceptibility is

$$\chi = [Ng^2\beta^2 S(S+1)/3k] [(1 + u_1 + u_2 + u_1 u_2)/(1 - u_1 u_2)] / (T - \theta) \quad (2)$$

with  $u_i = \coth[J_i S(S+1)/kT] - kT/[J_i S(S+1)]$  ( $i = 1, 2$ ), where  $J_1$  and  $J_2$  correspond to the alternating exchange constants for the EO and EE superexchange pathways, respectively, and the  $\theta$  parameter is included to correct

interchain antiferromagnetic interactions and/or zero-field splitting of the Mn(II) ion. By fixing the  $g$  parameter as the expected value of 2.0 for Mn(II), the best fit of the experimental data led to  $J_1 = 5.6(4) \text{ cm}^{-1}$ ,  $J_2 = -11.9(1) \text{ cm}^{-1}$ , and  $\theta = -1.2(1) \text{ K}$ . The  $J_1$  and  $J_2$  parameters confirm alternating F and AF interactions with the AF one dominating. Some important structural and magnetic parameters for 1D Mn–azido complexes with double EO and/or double EE bridges have been collected in our recent article.<sup>6</sup> Compound **3**, with comparable structural and magnetic data, follows the general trends reported therein.

## Conclusions

With two pyrazolylmethylpyridine bidentate ligands, three 1D Cu(II) and Mn(II) coordination polymers (**1–3**) with different azido-bridging networks have been prepared and characterized crystallographically and magnetically. It is difficult to predict the structure and magnetism of the metal–azido complex with a specific coligand, mainly due to the great diversity of the azido ion in bridging metal ions. For Cu(II), the situation is further complicated by its variable coordination number and geometry. Furthermore, in a given geometry for Cu(II) ions, the azido ion may occupy the axial or equatorial (basal) position, leading to different structures and magnetic properties. In the present case, compounds **1** and **2**, with very similar coligands and synthetic procedures, are distinct from each other in composition, topology, and magnetic property. Compound **1** is the second complex with alternate single EE and single EO azido bridges, and the intrachain interactions are ferromagnetic, just opposite those for the previously reported compound. Compound **2** exhibits an unprecedented “chain of rings” topology containing three different kinds of EO azido bridges: four Cu(II) ions are alternately bridged by single and double EO bridges to form a tetranuclear cyclic ring, and neighboring rings are interlinked by double EO bridges to generate a unique chain. This difference between **1** and **2** is a new demonstration of the remarkable versatility of the azido ion in building new magnetic materials and illustrates the great challenges and opportunities in the fields of coordination chemistry and molecular magnetism. Compound **3** consists of 1D Mn(II) chains in which double EO and double EE bridges alternate and mediate ferromagnetic and antiferromagnetic interactions, respectively.

**Acknowledgment.** We are thankful for the financial support of NSFC (Nos. 20201009, 90201014, 20001002, and 20221101) and MOST (G19980613).

**Note Added after ASAP:** Due to a production error, the version of this paper posted ASAP on November 6, 2003, contained an incorrect list of main IR bands for complex **3**. The version posted on November 13, 2003, contains the correct information.

**Supporting Information Available:** X-ray crystallographic file in CIF format. This material is available free of charge via the Internet at <http://pubs.acs.org>.

(27) (a) Manikandan, P.; Muthukumar, R.; Thomas, K. R. J.; Varghese, B.; Chandramouli, G. V. R.; Manoharan, P. T. *Inorg. Chem.* **2001**, *40*, 2378. (b) Costes, J. P.; Dahan, F.; Ruiz, J.; Laurent, J. P. *Inorg. Chim. Acta* **1995**, *239*, 53. (c) Costés, R.; Urriaga, M. K.; Lezama, L.; Larramendi, J. I. R.; Arriortua, M. I.; Rojo, T. *Dalton Trans.* **1993**, 3685.

(28) (a) Escuer, A.; Goher, M. A. S.; Mautner, F. A.; Vicente, R. *Inorg. Chem.* **2000**, *39*, 2107. (b) van Albada, G. A.; Lakin, M. T.; Veldman, N.; Spek, A. L.; Reedijk, J. *Inorg. Chem.* **1995**, *34*, 4910. (c) von Seggern, I.; Tuczck, F.; Bensch, W. *Inorg. Chem.* **1995**, *34*, 5530. (d) Kahn, O.; Sikorav, S.; Gouteron, J.; Jeannin, S.; Jeannin, Y. *Inorg. Chem.* **1983**, *22*, 2871. (e) Cortés, R.; Lezama, L.; Larramendi, J. I. R.; Insausti, M.; Folgado, J. V.; Madariaga, G.; Rojo, T. *Dalton Trans.* **1994**, 2573. (f) Sikorav, S.; Bkouche-Waksman, I.; Kahn, O. *Inorg. Chem.* **1984**, *23*, 490.